Expression and Mutagenesis of Mammalian Cytosolic NADP$^+$-Specific Isocitrate Dehydrogenase†

Gary T. Jennings,‡ Karyl I. Minard, and Lee McAlister-Henn*

Department of Biochemistry, University of Texas Health Science Center, San Antonio, Texas 78284-7760

Received April 21, 1997; Revised Manuscript Received August 28, 1997⊗

ABSTRACT: Rat liver cytosolic NADP$^+$-specific isocitrate dehydrogenase (IDP2) was expressed in bacteria as a fusion protein with maltose binding protein (MBP). High levels of expression were obtained. The fusion protein was purified from bacterial lysates by affinity chromatography with an amylose resin and found to be catalytically active. IDP2 was separated from MBP by cleavage with protease Xa and purified to homogeneity by FPLC anion-exchange chromatography. A specific activity of 56.3 units/mg and respective apparent K_m values for DL-isocitrate and NADP$^+$ of 9.7 ± 2.9 μM and 11.5 ± 0.2 μM were obtained for the purified enzyme. These values are similar to those previously reported for cytosolic isocitrate dehydrogenase isolated from a variety of tissues. Evolutionarily conserved arginine residues implicated in substrate binding were changed to glutamate residues using PCR based site-directed mutagenesis of the bacterial fusion plasmid. Mutant enzymes containing residue changes of R100E, R109E, R119E, or R132E were expressed, purified, and characterized by initial rate kinetic analyses. The R119E and R109E mutant enzymes exhibited respective 15- and 31-fold increases in K_m values for DL-isocitrate relative to the wild-type enzyme. In contrast, K_m values for NADP$^+$ were, respectively, unchanged and increased 9-fold. The most significant reductions in k_{cat}/K_m values were obtained for the R100E, R109E, and R132E enzymes. These results suggest that substrate binding residues are highly conserved between bacterial and mammalian enzymes despite low overall homology.

Three isozymes catalyze the oxidative decarboxylation of isocitrate to α-ketoglutarate in eucaryotic organisms. These isozymes differ in subcellular localization and cofactor specificity and are encoded by different genes. Mitochondria contain both NAD$^+$- and NADP$^+$-specific isocitrate dehydrogenases (EC 1.1.1.41 and EC 1.1.1.42), and the cytosol contains an NADP$^+$-specific isozyme. In mammals, the distribution of NADP$^+$-specific enzyme activity between the two cellular compartments varies in a tissue-specific manner. This activity is primarily cytosolic in ovary, mammary gland, and liver whereas the mitochondrial activity is predominant in heart and skeletal muscle (*1*−*5*). A small percentage of total cellular activity in liver is also reportedly associated with peroxisomal fractions (*6*).

NAD$^+$-specific isocitrate dehydrogenase is an octomer composed of two or three different types of subunits (*7*, *8*). It is allosterically responsive to energy charge and catalyzes a key regulatory step in the tricarboxylic acid cycle (*9*, *10*). The NADP$^+$-specific isozymes are homodimers whose metabolic functions are less well-defined. Analyses of yeast mutants containing various combinations of gene disruptions (*11*) suggest that the NADP$^+$-specific isozymes are essential for α-ketoglutarate production (and glutamate synthesis) in the absence of the NAD$^+$-specific enzyme and probably contribute to this function even in the presence of the latter enzyme. The inducible expression of mammalian cytosolic NADP$^+$-specific isocitrate dehydrogenase in ovary at the onset of ovulation (*12*, *13*) and in mammary gland during lactation (*14*) also suggests a potential function in supply of NADPH to support rapid rates of lipid synthesis.

The *Escherichia coli* gene encoding NADP$^+$-specific isocitrate dehydrogenase has been cloned (*15*) and the protein analyzed by X-ray crystallography (*16*). The aligned primary sequences of the bacterial and mammalian NADP$^+$-specific enzymes demonstrate a relatively low 14−24% residue identity, depending on alignment parameters (*17*, *18*). However, most of the residues in the bacterial enzyme known to participate in binding isocitrate−Mg^{2+} (*19*) are conserved in similar relative positions in the eucaryotic enzymes. In mammalian cytosolic NADP$^+$-specific isocitrate dehydrogenase, these residues correspond to Arg-109, Arg-132, Tyr-139, Lys-212, Asp-275, Asp-279, and Glu-304. In the current study, we examine the functional roles of three conserved residues in the mammalian enzyme.

EXPERIMENTAL PROCEDURES

Materials. Oligonucleotides were synthesized by the Center for Advanced DNA Technologies, University of Texas Health Science Center, San Antonio. Plasmid pMAL-c2 and *E. coli* strain TB1 were obtained from New England Biolabs (Beverly, MA), plasmid pCR II and *E. coli* strain INVFα from Invitrogen (San Diego, CA), plasmid pBS(−) from Stratagene (LaJolla, CA), and *E. coli* strain DH5αF′ from Clontech (Palo Alto, CA).

Vector Construction. To subclone rat liver *IDP2* for expression, polymerase chain reaction (PCR) techniques were used to amplify the full coding region extending from nucleotides 1 to 1245 and to add 5′ *Eco*RI and 3′ *Bam*HI restriction sites. Template DNA for PCR was a plasmid containing a 1.72 kbp *IDP2* cDNA fragment (*18*). The

† This work was supported by U.S. Public Health Service Grant GM51265 from the National Institutes of Health.

* Corresponding author.

‡ Present address: TVW Telethon Institute for Child Health Research, West Perth, WA 6872, Australia.

⊗ Abstract published in *Advance ACS Abstracts,* October 15, 1997.

S0006-2960(97)00916-1 CCC: $14.00

reaction contained 100 μL of 10 mM Tris-HCl (pH 8.3), 50 mM NaCl, 1.5 mM $MgCl_2$, 0.2 mM dNTPs, 1 mM each oligonucleotide primer (5′TTTGAATTCATGTCCA-GAAAAATCCATGGC and 5′CTAGAGGATCCCTAT-TAAAGTTTGGCCTGAGCTAG), and 2.5 units of *Ampli-Taq* DNA polymerase (Perkin Elmer, Foster City, CA). Denaturation, annealing, and polymerization reactions were performed at 94 °C for 5 min, 65 °C for 2 min, and 72 °C for 2 min, respectively. The cycle was repeated 24 times. The PCR product was subcloned into plasmid pCR II using a TA cloning kit (Invitrogen), and then transferred into the multicloning site of plasmid pMAL-c2 using *Eco*RI and *Bam*HI sites. The fidelity of PCR amplification was confirmed by dideoxynucleotide sequence analysis (*20*) of the entire *IDP2* coding region. Bacterial transformation, plasmid amplification, and ligation were performed as described by Sambrook *et al*. (*21*).

Site-directed mutagenesis was performed using the two-step PCR procedure of Ito *et al*. (*22*) with oligonucleotides to generate R100E (5′GGAAATCACCCAACGGAACCATC-GAGAACATTCTGGGCG), R109E (5′GATAATAGCT-TCTTCGAAGACAGTGCC), R119E (5′CTGTCACTAG-CTCGGGGATATTTTTGC), or R132E codon changes (5′CATAGGCGTGCTCGCCAATGATGATGG). This procedure limited amplification to a 307 bp *Bst*EII/*Pfl*MI restriction fragment. Mutations were confirmed by sequence analysis of the fragments prior to subcloning into the pMAL-*IDP2* plasmid.

Expression and Purification of IDP2. *E. coli* TB1 cells transformed with pMAL-*IDP2* were grown at 30 °C to an $A_{600nm} = 0.5$ in Luria Broth medium containing 50 μg/mL ampicillin and 2 g/L glucose. Isopropyl thiogalactoside was added to a final concentration of 0.3 mM, and the cultures were incubated an additional 2 h. Cells were collected by centrifugation at 4000*g* for 10 min and resuspended (0.1 g/mL) in buffer A containing 20 mM Tris-HCl (pH 7.4), 200 mM NaCl, 1 mM EDTA, and 10% (w/v) glycerol. The cell suspension was lysed by sonication and debris removed by centrifugation at 9000*g* for 25 min. The supernatant was diluted 4-fold with buffer A and applied (12 mL/g of resin) to an amylose resin column (New England Biolabs, Beverly, MA) at a flow rate of 1 mL/min. The column was washed with 10 column volumes of buffer A and the MBP−IDP2 fusion protein eluted with buffer A containing 10 mM maltose. The fusion protein was digested for 12 h at 4 °C with factor Xa (1 μg/200 μg of fusion protein) and dialyzed for 8 h at 4 °C against 150 volumes of buffer B (20 mM triethanolamine−NaOH, pH 7.6, and 10% glycerol). FPLC anion exchange chromatography was conducted using a mono Q (HR 5/5) column (Pharmacia, Piscataway, NJ) equilibrated with buffer B. Protein (1−2 mg) applied to the column was eluted with a continuous salt gradient (0−250 mM NaCl in buffer B) at a flow rate of 0.5 mL/min. Fractions from each stage of the purification were used for enzyme assays and electrophoretic analyses.

Enzyme and Protein Assays. For purification, IDP2 activity was assayed at 25 °C in 1.0 mL reactions containing 0.1 M Tris-HCl (pH 8.0), 3 mM $MgCl_2$, 0.5 mM $NADP^+$, and 10% (w/v) glycerol. The reaction was initiated by adding DL-isocitrate to a final concentration of 1.5 mM and the rate of NADPH production measured spectrophotometrically at 340 nm. Protein concentrations were determined by the Ponceau S method of Pesce and Strande (*23*) using bovine serum albumin as the standard. Units are expressed as micromoles of NADPH formed per minute per milligram of protein. For kinetic analyses, the concentration of $NADP^+$ was varied from 10 μM to 1.0 mM with a saturating concentration of 1.5 mM DL-isocitrate, or the concentration of DL-isocitrate was varied from 10 μM to 2 mM with a concentration of 0.5 mM $NADP^+$. The concentration of enzyme in assays was 0.5−1.0 μg/mL.

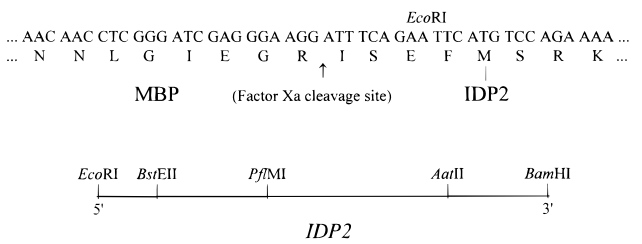

FIGURE 1: Sequences at the point of fusion between MBP and IDP2 and partial restriction map of *IDP2*. The *IDP2* coding region was amplified by PCR with 5′ *Eco*RI and 3′ *Bam*HI restriction sites introduced for subcloning into the bacterial expression plasmid pMAL-c2. Expression produces a fusion protein with the carboxy terminus of MBP linked to the amino terminus of IDP2 by a peptide containing the factor Xa protease recognition sequence (IEGR). The site of factor Xa cleavage (↑) and the authentic amino terminus of IDP2 (|) are indicated. The restriction map indicates sites utilized in subcloning.

Electrophoretic Methods. Discontinuous sodium dodecyl sulfate (SDS)−polyacrylamide gel electrophoresis was conducted using the procedure of Laemmli and Favre (*24*) with 10% (w/v) polyacrylamide separating gels (pH 8.8) and 4% (w/v) polyacrylamide stacking gels (pH 6.8). Immunoblot analyses were conducted as previously described (*25*) using an antiserum prepared against purified IDP2 from porcine corpora lutea. Immunoreactive polypeptides were detected using the enhanced chemiluminescent method and autoradiography.

RESULTS AND DISCUSSION

Expression and Purification of Recombinant IDP2. For expression in bacteria, PCR was used to amplify the 1245 bp coding region for $NADP^+$-specific isocitrate dehydrogenase (IDP2) using as template a plasmid containing the 1.72 kbp *IDP2* cDNA from a rat liver library (*18*). The *IDP2* coding region was subcloned to produce an in-frame fusion with the 3′ end of the coding region for maltose binding protein (MBP, Figure 1) in the expression plasmid pMAL-c2. Complete nucleotide sequence analysis of the cloned PCR product in pMAL-*IDP2* revealed a single PCR-generated error, a G to C substitution at nucleotide position 685. This error was corrected by replacing a 500 bp *Pfl*MI/*Aat*II restriction fragment in pMAL-*IDP2* (Figure 1) with the corresponding fragment from the authentic cDNA. However, the plasmid containing the PCR error, which results in replacement of the codon for Glu-229 by a codon for lysine, was retained as a control for nonspecific mutagenesis.

Plasmid pMAL-*IDP2* was transformed into *E. coli* strain TB1. Conditions for optimal expression were determined empirically. These included growth of cultures at 30 °C to low density and induction of the *tac* promoter with isopropyl thiogalactoside for 2 h prior to harvesting the cells. The MBP−IDP2 fusion protein was purified from cell lysates using amylose affinity chromatography. Based on recovery

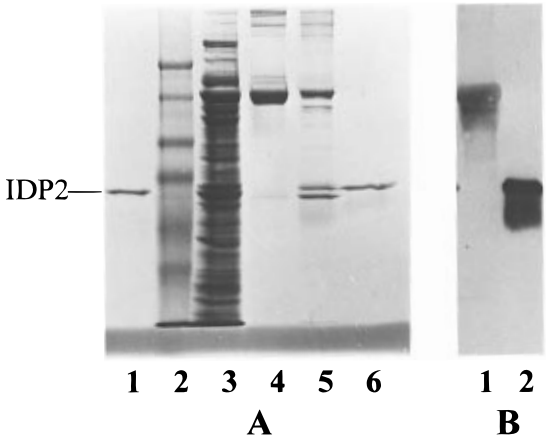

FIGURE 2: Electrophoretic analyses of the purification of recombinant IDP2. Samples from each step in the purification of IDP2 were electrophoresed on a polyacrylamide−sodium dodecyl sulfate gel and stained with Coomassie blue (panel A). Samples included conventionally purified enzyme from rat ovary (lane 1, 1 μg; *25*), prestained protein molecular weight standards (lane 2), sonicate from bacterial cells following induction of expression (lane 3, 20 μg), eluate from amylose resin (lane 4, 2 μg), eluate following protease Xa cleavage (lane 5, 2 μg), and a fraction following monoQ chromatography (lane 6, 1 μg). Immunoblot analysis (panel B) was conducted with the amylose resin eluate (lane 1) and purified recombinant IDP2 (lane 2) using an antiserum prepared against purified mammalian IDP2 as described under Experimental Procedures.

from the sonicate at this step, the protein is expressed to levels representing approximately 20% of the total protein. The purified fusion protein, upon analysis by denaturing SDS−polyacrylamide gel electrophoresis (Figure 2A, lane 4), is of the size predicted from the sum of molecular weights for MBP (43 000) and IDP2 polypeptides (47 000) and, when subjected to cleavage by factor Xa protease, yields polypeptide bands of these sizes (Figure 2A, lane 5). The fusion protein and larger polypeptide cleavage product are immunoreactive with antiserum specific for IDP2 (Figure 2B, lanes 1 and 2, respectively). The fusion protein and smaller polypeptide cleavage product are immunoreactive with antiserum specific for MBP (data not shown).

Enzyme assays conducted with bacterial cell lysates indicate an increase in $NADP^+$-specific isocitrate dehydrogenase activity of 3.3-fold relative to endogenous levels measured for lysates from noninduced cultures. The purified fusion protein was determined to have a specific activity of 31.3 units/mg. Furthermore, the apparent K_m of the MBP−IDP2 fusion protein for DL-isocitrate was determined to be 16.9 μM, a value similar to the 9.7 μM measured for the purified recombinant enzyme. These results indicate that the IDP2 portion of the MBP−IDP2 fusion protein is properly folded and can adopt an active dimeric conformation.

Following factor Xa cleavage, IDP2 was purified from MBP and residual MBP−IDP2 by FPLC anion exchange chromatography as described under Experimental Procedures. The purified enzyme appears to be homogeneous, as judged by SDS−polyacrylamide gel electrophoresis (Figure 2A, lane 6). The two-step scheme resulted in a 10.7-fold purification of IDP2 from the bacterial sonicate. A low yield of purified enzyme (approximately 3%) was accepted to restrict factor Xa cleavage to approximately 10% and to eliminate collection of column fractions with less than maximal IDP2 activity. The purified recombinant enzyme has a specific activity of 56.3 units/mg, a value similar to those reported for IDP2 purified from porcine ovary, rat liver, and bovine mammary gland (*25*−*27*). This indicates that addition of four amino acid residues to the authentic amino terminus of IDP2, a result of the fusion protein construction and cleavage (Figure 1), is not detrimental to catalytic activity.

With this expression system, the MBP−IDP2 fusion protein is soluble and exhibits significant dehydrogenase activity. We also recently reported use of the same system for expression of mammalian mitochondrial $NADP^+$-specific isocitrate dehydrogenase (*28*) which shares a 70% residue identity with IDP2 (*18*). In that case, catalytic activity was not apparent for the fusion protein but was regained following protease cleavage. Also, the mitochondrial protein proved to be susceptible to internal cleavage with protease Xa, and it was necessary to introduce an alternative thrombin cleavage site for successful purification. Similar specific activities and K_m values were obtained for the purified recombinant mammalian enzymes.

Expression and Kinetic Analyses of Mutant Variants of IDP2. As described above, the primary sequences of *E. coli* isocitrate dehydrogenase (ICD) and of eucaryotic $NADP^+$-specific isocitrate dehydrogenases show little relatedness despite similarities in polypeptide sizes, cofactor specificity, and dimeric structures. In fact, ICD is much more similar in sequence with the subunits of eucaryotic NAD^+-specific enzymes (*29*, *30*). However, within aligned sequences of the $NADP^+$-specific enzymes are regions of homology, particularly in areas around conserved residues known to participate in substrate binding in the bacterial enzyme (*19*). To test the functional relevance of this structural conservation, we have focused on a relatively homologous region (Figure 3) bordered by bacterial Ser-113, a residue critical for isocitrate binding and catalysis (*15*), and Tyr-160, a residue with an important role in the dehydrogenation step in catalysis (*31*, *32*). The most optimal alignment (I) within this region demonstrates conservation of these residues as Ser-94 and Tyr-139 in mammalian IDP2 but differs from an alignment (II) obtained by Clustal analysis of multiple sequences (*17*). Between these residues in the bacterial sequence is a cluster of arginine residues that form hydrogen bonds with carboxyl groups of isocitrate. To test possible functional conservation of this cluster, site-directed mutagenesis was used to introduce R100E, R109E, and R132E changes in corresponding codons in the *IDP2* coding region. Additionally, Arg-119 in IDP2, which lacks a homologue in alignment I (Figure 3), was also targeted for mutagenesis by introduction of an R119E codon change. Codon changes were introduced by a two-step PCR procedure to limit mutagenesis and amplification to a 307 bp *Bst*EII/*Pfl*MI restriction fragment (Figure 1). The PCR products were used to replace the same fragment in pMAL-*IDP2*, and the region was sequenced to ascertain that only the desired changes were introduced.

Plasmids containing the R100E, R109E, R119E, or R132E mutations, as well as the E229K mutation obtained as a cloning artifact as described above, were transformed into bacterial strain TB1 for expression as MBP fusion proteins. The fusion proteins were purified using amylose columns, treated with factor Xa, and the mutant proteins isolated following FPLC chromatography as described above for the wild-type enzyme. The only differences noted during purification were altered elution profiles in the anion

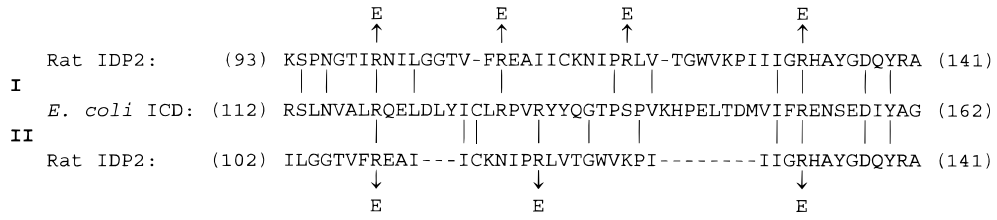

FIGURE 3: Comparison of amino acid sequences for *E. coli* isocitrate dehydrogenase (ICD) and rat IDP2 in a region containing several residues of the bacterial enzyme involved in substrate binding. Alignment I minimizes gaps; alignment II was obtained in a multisequence comparison (*17*). Residue identities (|) and IDP2 residues targeted for mutagenesis (↑) are indicated.

Table 1: Kinetic Characteristics of Wild-Type and Mutant Forms of Recombinant IDP2

	enzyme					
kinetic characteristic[a]	wild-type	E229K	R100E	R109E	R119E	R132E
V_{max} (units/mg)	56.3	56.5	0.07	0.35	56.3	0.03
K_m(NADP$^+$) (μM)	11.5	10.0	ND[b]	104	8.3	ND
K_m (DL-isocitrate) (μM)	9.7	16.7	ND	303	145	ND
k_{cat}	88.2	88.5	0.11	0.55	88.2	0.05
k_{cat}/K_m (isocitrate) (s^{-1} M^{-1})	9.1×10^6	5.3×10^6	1.1×10^4 [c]	1.8×10^3	6.1×10^5	5.2×10^3 [c]
relative k_{cat}/K_m	1.0	0.6	1.2×10^{-3} [c]	2×10^{-4}	0.07	5.7×10^{-4} [c]

[a] Assays were conducted as described under Experimental Procedures. [b] Values not determined. [c] Values were calculated using the K_m value for DL-isocitrate of the wild-type enzyme.

exchange step, presumably reflecting charge differences of the mutant enzymes. Final yields and purity of mutant enzymes were similar to those obtained for the recombinant wild-type enzyme. Enzyme assays conducted following purification indicated particular lability upon storage at 4 °C of the R109E mutant enzyme, which exhibited an activity half-life of 10 h relative to half-lives greater than 48 h for the wild-type and other mutant enzymes. Therefore, kinetic characterizations were performed immediately after the FPLC purification steps.

Table 1 summarizes kinetic properties measured for recombinant IDP2 and mutant forms of the enzyme. Despite a dramatic charge change, the E229K replacement as expected does not appear to affect catalytic activity. In contrast, the significant effects of R100E, R109E, and R132E replacements on the kinetic properties of IDP2 are consistent with direct functions of these residues in substrate binding. The R100E and R132E enzymes are essentially catalytically inactive. The k_{cat}/K_m value for isocitrate for the R109E enzyme is reduced by more than 3 orders of magnitude relative to the wild-type enzyme. The additional 9-fold increase in K_m for NADP$^+$ for the R109E enzyme may be due to local effects on hydride transfer between isocitrate and cofactor as reported for mutant bacterial enzymes containing residue replacements for Tyr-160 (*31*, *32*). Overall, these results are consistent with alignment I in Figure 3 and suggest that Arg-100, Arg-109, and Arg-132 in IDP2 are, respectively, homologues of bacterial Arg-119, Arg-129, and Arg-153. These results also support the conclusion from crystallographic studies that side chains of these residues form hydrogen bonds with the α- and/or β-carboxyl groups of isocitrate (*19*).

The replacement of Arg-119, which has no homologue in the bacterial sequence, with glutamate has a more moderate effect on activity, producing a 14.9-fold increase in the K_m for isocitrate but no effect on the apparent affinity for NADP$^+$ or on k_{cat}. This could be due to proximity to other active site residues rather than to a direct effect. Alternatively, the R119E mutation may stabilize some conformation of the enzyme that is less conducive to isocitrate binding. The *E. coli* enzyme demonstrates small conformational differences when bound with α-ketoglutarate as compared to isocitrate (*33*), and the homologous NAD$^+$-specific isopropylmalate dehydrogenase undergoes loop closing upon binding of cofactor (*34*). These differences do not involve large domain movements but do indicate the existence of distinct open and closed structures.

The only other reported mutagenesis analyses of eucaryotic isocitrate dehydrogenases have focused on homologues of the *E. coli* Ser-113 residue. That residue in the bacterial enzyme participates in isocitrate binding and is the site for *in vivo* phosphorylation which inactivates the enzyme (*15*). The phosphorylation of ICD is an important regulatory mechanism for redirecting carbon flux from the tricarboxylic acid cycle into the biosynthetic glyoxylate pathway (*35*). Replacement of Ser-113 with an aspartate residue produces an inactive bacterial enzyme (*15*). Similar alteration of homologues of Ser-113 in the two subunits of yeast NAD$^+$-specific isocitrate dehydrogenase was used to clarify catalytic and regulatory functions of each subunit (*36*). Also, a homologous S94D replacement in yeast mitochondrial NADP$^+$-specific isocitrate dehydrogenase, which shares over 50% residue identity with mammalian IDP2, results in an enzyme with no measurable catalytic activity *in vitro* or *in vivo* but that retains its dimeric structure (*37*). These results, in combination with those obtained in the current study, suggest that the catalytic mechanisms of the NADP$^+$-specific enzymes from bacterial and eucaryotic sources are very similar despite their significant evolutionary divergence.

ACKNOWLEDGMENT

We thank Mr. Dejun Xuan for his assistance in constructing and expressing mutant enzymes, and Dr. Paul Horowitz and members of his laboratory for use of FPLC chromatography equipment.

REFERENCES

Farrell, H. M., Jr., Deeney, J. T., Tubbs, K., & Walsh, R. A. (1987) *J. Dairy Sci. 70,* 781−788.

Flint, A. P. F., & Denton, R. M. (1970) *Biochem. J. 117*, 73−83.
Henderson, N. S. (1968) *Ann. N.Y. Acad. Sci. 151*, 429−440.
Hogeboom, G. H., & Schneider, W. C. (1950) *J. Biol. Chem. 186*, 417−427.
Plaut, G. W. E., Cook, M., & Aogaichi, T (1983) *Biochim. Biophys. Acta 760*, 300−308.
Leighton, F., Poole, B., Beaufay, H., Baudhuin, P., Coffey, J. W., Fowler, S., & DeDuve, C. (1968) *J. Cell Biol. 37*, 482−513.
Keys, D. A., & McAlister-Henn, L. (1990) *J. Bacteriol. 172*, 4280−4287.
Plaut, G. W. E. (1970) in *Current Topics in Cellular Regulation 2* (Horeker, B. L., and Stadtman, E. R., Eds.) pp 1−27, Academic Press, New York.
Hathaway, J. A., & Atkinson, D. E. (1963) *J. Biol. Chem. 238*, 2875−2881.
Barnes, L. D., McGuire, J. J., & Atkinson, D. E. (1972) *Biochemistry 11*, 4322−4328.
Zhao, W.-N., & McAlister-Henn, L. (1996) *Biochemistry 35*, 7873−7878.
Klinken, S. P., & Stevenson, P. M. (1977) *Eur. J. Biochem 81*, 327−332.
Jennings, G. T., & Stevenson, P. M. (1991) *Eur. J. Biochem. 198*, 621−625.
Baldwin, R. L. (1966) *J. Dairy Sci. 49*, 1533−1542.
Thorsness, P. E., & Koshland, D. E., Jr. (1987) *J. Biol. Chem. 262*, 10422−10425.
Hurley, J. H., Thorsness, P. E., Ramalingam, V., Helmers, N. H., Koshland, D. E., Jr., & Stroud, R. E. (1989) *Proc. Natl. Acad. Sci. U.S.A. 86*, 8635−8639.
Haselbeck, R. J., Colman, R. F., & McAlister-Henn, L. (1992) *Biochemistry 31*, 6219−6223.
Jennings, G. T., Sechi, S., Stevenson, P. M., Tuckey, R. C., Parmelee, D., & McAlister-Henn, L. (1994) *J. Biol. Chem. 269*, 23128−23134.
Hurley, J. H., Dean, A. M., Koshland, D. E., Jr., & Stroud, R. M. (1991) *Biochemistry 30*, 8671−8678.
Sanger, F., Nicklen, S., & Coulson, A. R. (1977) *Proc. Natl. Acad. Sci. U.S.A. 74*, 5463−5467.
Sambrook, J., Fritsch, E. F., & Maniatis, T. (1989) in *Molecular Cloning: a Laboratory Manual* (Ford, N., Ed.) 2nd ed., Cold Spring Harbor Laboratory Press, Cold Spring Harbor, NY.
Ito, W., Ishiguro, H., & Kurosawa, Y. (1991) *Gene 102*, 67−70.
Pesce, M. A., & Strande, C. S. (1973) *Clin. Chem. 19*, 1265−1267.
Laemmli, U. K., & Favre, M. (1973) *J. Mol. Biol. 80*, 575−599.
Jennings, G. T., Sadleir, J. W., & Stevenson, P. M. (1990) *Biochim. Biophys. Acta 1034*, 219−227.
Farrell, H. M., Jr. (1980) *Arch. Biochem. Biophys. 204*, 551−559.
Carlier, M. F., & Pantaloni, D. (1973) *Eur. J. Biochem. 37*, 341−354.
Soundar, S., Jennings, G. T., McAlister-Henn, L., & Colman, R. F. (1996) *Protein Expression Purif. 8*, 305−312.
Cupp, J. R., & McAlister-Henn, L. (1991) *J. Biol. Chem. 266*, 22199−2225.
Cupp, J. R., & McAlister-Henn, L. (1992) *J. Biol. Chem. 267*, 16417−16423.
Lee, M. E., Dyer, D. H., Klein, O. D., Bolduc, J. M., Stoddard, B. L., & Koshland, D. E., Jr. (1995) *Biochemistry 34*, 378−384.
Bolduc, J. M., Dyer, D. H., Scott, W. G., Singer, P., Sweet, R. M., Koshland, D. E., Jr., & Stoddard, B. L. (1995) *Science 268*, 1312−1318.
Stoddard, B. L., & Koshland, D. E. Jr., (1993) *Biochemistry 32*, 9317−9322.
Hurley, J. H., & Dean, A. M. (1994) *Structure 15*, 1007−1016.
LaPorte, D. C., & Koshland, D. E., Jr. (1983) *Nature 305*, 286−290.
Cupp, J. R., & McAlister-Henn (1993) *Biochemistry 32*, 9323−9328.
Haselbeck, R. J. (1993) Ph.D. Dissertation, University of California, Irvine, CA.

BI970916R